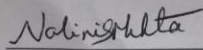


LMC 4702-Research Proposal-Malvika Sanghvi

Cover Page

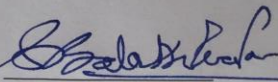
**Potential Therapy against Glioblastoma using Motile  
Nanocarrier Expressing TRAIL and Azurin**

Signature:



Dr. Nalini Mehta

Signature:



Dr. Balakrishna Pai

# **Potential therapy against Glioblastoma using Motile Nanocarrier**

## **Expressing TRAIL and Azurin**

Malvika Sanghvi, Dr. Nalini Mehta, Dr. Bellamkonda(PI)

### **Abstract**

Glioblastoma (GBM) is the most common and aggressive type of gliomas in humans. It is also highly resistant to most treatment methods. Nearly 12,000 people are diagnosed with glioblastoma each year in the United States. Approximately two out of three glioblastoma patients will fail today's approved therapies. The tumor grows by changing normal brain cells to stem cell, which can continuously replicate and regrow a tumor with only a handful of cells left behind. In this paper we research two different methods to approach the problem. The first method 1) Cloning soluble TRAIL into plasmid with hypoxic promoter and transforming into avirulent *Salmonella Typhimurium* for inducing apoptosis in Glioblastoma cells and the second method is 2) To check if avirulent *Salmonella Typhimurium* seeks tumors and expresses proteins such as Azurin. This paper demonstrates the qualitative results of both.

### **Introduction & Background**

The main obstacle faced in treating GBM is in delivery, in that, inconsistency in diffusion gradient because of inefficient diffusion through solid tumors. The current treatment option called convection enhanced diffusion (CED) tackles this problem by introducing the drug at high pressure into the tumor. However this leads to side effects such as inflammation due to the high pressure.

The main principle of this treatment is to deliver a gene drug via a cationic liposomal vector using liposomes as vehicles. CED helps to transport particles over long distances creating reasonably high tissue concentrations within large volumes. Also, using liposomes as vehicles, instead of viral vectors, is a huge advantage. This is because of their uncomplicated preparation and application, the lack of immunogenicity and safety requirements, and their comparably long stability at room temperature. Safety and efficacy of intracerebrally infused cationic liposome gene constructs have been investigated experimentally in vivo and have been chosen for clinical application. However, although the method is non-invasive, the process of diffusion has its side-effects. Intracranial pressure leads to neural edema, which is inflammation of the brain.<sup>8</sup> Further, this method of treatment is not efficient either- diffusion does not guarantee uniform distribution or penetration of the drug to all affected necrotic regions in the brain. This is also a cause for relapse of the glioma.

The other dire problem in the field of anti-cancer drugs is that of clinical attrition. The rates for cancer are much higher than those for any other disease because of the complexities involved in identifying the correct target using the suitable models.<sup>9</sup> Therefore there is a serious need for developing therapies that address all the gaps in the relevant research mentioned above. That is how the concept of navigated drug delivery mediated by a molecular ‘vehicle’ has come about. This ‘vehicle’ is required to have a) the transporting vehicle (i.e., lipid), b) the loaded cytotoxic agent, and c) the “programmable” navigating/targeting agent (i.e., receptor specific ligand) that enables the appropriate delivery routes to avoid toxicity on healthy cells. The ineffective concentration of the cytotoxic agent, and the “stealth” nanocarriers (biocompatibility polymers,

i.e., PEG) enhance the short plasma half-life of the drug-loaded transporting vehicle.<sup>10</sup> These components are imperative in order for the drug to be able to improve the drug's selective uptake of the cytotoxic agent by the tumor cells, not harm healthy cells.

Hence one new potential treatment method that fulfills the purpose of delivery but also overcomes the pressure problem of CED is delivery of drug via a nano-carrier such as avirulent ST, which has high migratory and invasive potential.

For the first study, the protein that we are trying to get delivered into the cells-t is the TRAIL protein that is Tumor necrosis factor related apoptosis inducing ligand: a member of the tumor necrosis factor (TNF) family. It has high selectivity & specificity in targeting cancer cells for apoptosis. The only major downside is that many GBM tumors that make them resistant to TRAIL. So high concentrations of TRAIL would be required to induce apoptosis.

For the second study, the objective is to verify if ST is actually tumor seeking and whether or not it will express proteins Azurin. Hypoxia is characteristic of necrotic regions in the brain. Furthermore, when normal cells start dying, they spill all of their organelles in the region and hence, this region becomes rich in “nutrients”. The ST used is made to be immunocompromised, that is, it is devoid of its lipid A layer, which is responsible for providing the bacterium with its nutrients and purines. This is done to fulfill the aim of checking whether the bacteria travel to the necrotic region. A summary of the he protein, Azurin, are given in Table 1.

Description	Very small protein (cupredoxin) produced by several pathogens, for ex. <i>Pseudomonas aeruginosa</i>
Function	Inhibits angiogenesis in cancer cells through inhibition of the phosphorylation of VEGFR-2, FAK, and AKT.
Mechanism/Pathway	Binds to p53, stabilizes it and prevents proteasome degradation by inhibiting ubiquitination
Anti-cancer properties	<ul style="list-style-type: none"> <li>•Highly selective and specific: ability to preferentially enter cancer cells without harming healthy neighbor cells</li> <li>•Prevents cancer growth : Extrinsic apoptosis by forming DISC complexes with key proteins involved in cancer growth promoters</li> </ul>

**Figure 1. Azurin**

## Approved Work Plan

My work attempts to bridge these gaps, by eliminating as many drawbacks as possible. I begin by establishing the prominence of the disease and the causes associated with it. Next, I explain the current treatment options and critique them briefly. Finally, I outline my approach to the problem and explain how it eliminates the problems with the current treatments

## Methods and materials

Experiment 1) A series of molecular biology laboratory techniques were followed to transform the bacteria with the customized vector. Further, the bacteria was inject in Fischer rats, made hosts to the U87-MG cancer cell line. The plasmid vector has a secretory signal peptide, IgK(Immunoglobulin Kappa), a hypoxic promoter which functions only under hypoxic conditions, PfLE(Pyruvate formate-lyase enzyme), the protein of interest, TRAIL and the probe, GFP(Green

Fluorescent Protein) so that it fluoresces under a suitable wavelength of light. The GFP is downstream of TRAIL to see if the GFP is expressed along with TRAIL. After it is activated, the extrinsic pathway of apoptosis is initiated by binding to TRAIL-R1 and/or TRAIL-R2, whereupon the adaptor protein Fas-associated death domain (FADD) and initiator caspase-8 are recruited to the DD of these receptors. Assembly of this so-called death-inducing signaling complex leads to the sequential activation of initiator and effector caspases, and ultimately results in apoptotic cell death.

Experiment 2) A rat model of Fischer Rats was set up, on which *in vivo* studies were performed. A summary of the methods can be found in Table 2. Both, the control group as well as the subject group, were developed with GBM. After 10 days, the control group did not receive any drug, the IC group of rats received the drug intra-cranially from a hole in the right cortex, and finally, the IV group received the drug, injected through their spine, that is, intra-venous. Following this, the animals were sacrificed, perfused and then the brains were harvested and coronally sectioned. All the sections were made to undergo three different types of staining: 1) Immunohistochemical staining (IHC), 2) Fluorescence in situ hybridization (FISH) and, 3) Hematoxylin & Eosin stain (H & E).

CONTROL GROUP	SUBJECT GROUP I	SUBJECT GROUP II
FISCHER 28,29,30	FISCHER 21,23, 25	FISCHER 22,24,26
IC Tumor-both cortices	IC Tumor- both cortices	IC Tumor- both cortices
<ul style="list-style-type: none"> <li>After 10 days, saline was inject IC into right cortex</li> </ul>	<ul style="list-style-type: none"> <li>After 10 days, Salm strain that has Azurin plasmid was injected into right cortex (IC)</li> </ul>	<ul style="list-style-type: none"> <li>After 10 days, Salm strain that has Azurin plasmid was injected into tail vein (IV)</li> </ul>

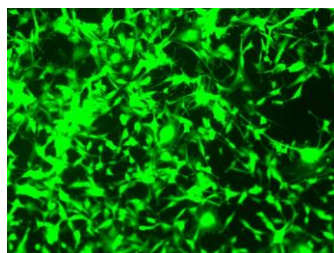
Figure 2. Fischer Rat Model for Experiment 2, in vivo studies for cell line

### 3RT1RT2A

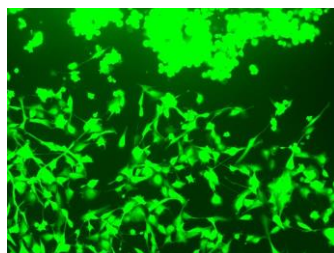
#### Results

Figure 1 are images to show the MRI slides of the *In vitro* Results: testing ST with GC PflE-IgK-TRAIL-GFP plasmid against U87MG-GFP cells. The last image shows the changes in morphology of the cells due to VNP plus plasmid. Figure 2 are images to show how the tumor developed inside the brains. A lot of heterogeneity as observed- some developed a tumor on the right cortex, some on the left and some, in both cortices. Next, Figure 3 shows images after FISH with dyes such as DAPI and Texas Red. The 21s chromosome of the bacteria DNA was hybridized by the artificially constructed FISH probe. In the images, the blue color represents the necrotic region and the red spots represent the bacteria. Therefore, the overlap of blue and red show that bacteria successfully reached the necrotic region and hence were actually tumor seeking. Further, Figure 4a and 4b show

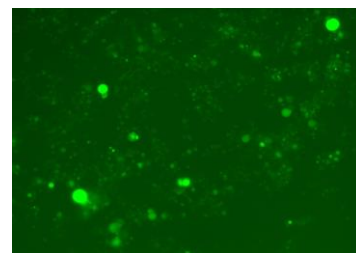
images for IHC. In this staining, we were staining for the hypoxic region with the primary antibody anti-Hif1- $\alpha$  raised in rabbit monoclonal IgG Ab from ABCAM-ab51608, and secondary antibody, raised in goat and was anti-mouse IgG1(fluoresces under 633nm). The second protein that was stained for was Flag, to track Azurin, This was done by primary antibody, anti-FLAG, raised in mouse monoclonal antibody IgG1 from SIGMA F 804, and secondary antibody, raised in oat anti-Rabbit IgG. An overlap of both these images were done and it showed that Azurin was produced in the hypoxic regions. Figure 5 shows images after H & E staining. This was done with the purpose of getting an overall picture of the tumor with respect to the brain. For these images, since the brain was not frozen in para and sucrose, we see lot of open regions due to ice crystal formation. The bacteria was not responsible for any activity there.



**U87MG cells  
No bacteria**



**U87MG cells-with VNP  
No plasmid**



**U87MG cells-with VNP plus Plasmid**

*Figure 1*



[illegible]

Figure 1 is an axial MRI scan of the head, showing a large, well-defined, hyperintense mass in the posterior fossa, consistent with a cerebellar tumor. The mass is causing significant mass effect and compression of the surrounding brain tissue. Technical parameters are visible on the left and right sides of the image.

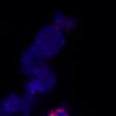
Morgan Tech  
 11/19/2019  
 1.2 kg

SI 5000.00 mm  
 PCV 50.00 mm  
 M15.00 mm  
 Pos 0.75 mm  
 Scale 1.00  
 F16.00 mm  
 F2.00 mm  
 F3.00 mm  
 F4.00 mm  
 F5.00 mm  
 F6.00 mm  
 F7.00 mm  
 F8.00 mm  
 F9.00 mm  
 F10.00 mm  
 F11.00 mm  
 F12.00 mm  
 F13.00 mm  
 F14.00 mm  
 F15.00 mm  
 F16.00 mm  
 F17.00 mm  
 F18.00 mm  
 F19.00 mm  
 F20.00 mm  
 F21.00 mm  
 F22.00 mm  
 F23.00 mm  
 F24.00 mm  
 F25.00 mm  
 F26.00 mm  
 F27.00 mm  
 F28.00 mm  
 F29.00 mm  
 F30.00 mm  
 F31.00 mm  
 F32.00 mm  
 F33.00 mm  
 F34.00 mm  
 F35.00 mm  
 F36.00 mm  
 F37.00 mm  
 F38.00 mm  
 F39.00 mm  
 F40.00 mm  
 F41.00 mm  
 F42.00 mm  
 F43.00 mm  
 F44.00 mm  
 F45.00 mm  
 F46.00 mm  
 F47.00 mm  
 F48.00 mm  
 F49.00 mm  
 F50.00 mm  
 F51.00 mm  
 F52.00 mm  
 F53.00 mm  
 F54.00 mm  
 F55.00 mm  
 F56.00 mm  
 F57.00 mm  
 F58.00 mm  
 F59.00 mm  
 F60.00 mm  
 F61.00 mm  
 F62.00 mm  
 F63.00 mm  
 F64.00 mm  
 F65.00 mm  
 F66.00 mm  
 F67.00 mm  
 F68.00 mm  
 F69.00 mm  
 F70.00 mm  
 F71.00 mm  
 F72.00 mm  
 F73.00 mm  
 F74.00 mm  
 F75.00 mm  
 F76.00 mm  
 F77.00 mm  
 F78.00 mm  
 F79.00 mm  
 F80.00 mm  
 F81.00 mm  
 F82.00 mm  
 F83.00 mm  
 F84.00 mm  
 F85.00 mm  
 F86.00 mm  
 F87.00 mm  
 F88.00 mm  
 F89.00 mm  
 F90.00 mm  
 F91.00 mm  
 F92.00 mm  
 F93.00 mm  
 F94.00 mm  
 F95.00 mm  
 F96.00 mm  
 F97.00 mm  
 F98.00 mm  
 F99.00 mm  
 F100.00 mm

SI 5000.00 mm  
 PCV 50.00 mm  
 M15.00 mm  
 Pos 0.75 mm  
 Scale 1.00  
 F16.00 mm  
 F2.00 mm  
 F3.00 mm  
 F4.00 mm  
 F5.00 mm  
 F6.00 mm  
 F7.00 mm  
 F8.00 mm  
 F9.00 mm  
 F10.00 mm  
 F11.00 mm  
 F12.00 mm  
 F13.00 mm  
 F14.00 mm  
 F15.00 mm  
 F16.00 mm  
 F17.00 mm  
 F18.00 mm  
 F19.00 mm  
 F20.00 mm  
 F21.00 mm  
 F22.00 mm  
 F23.00 mm  
 F24.00 mm  
 F25.00 mm  
 F26.00 mm  
 F27.00 mm  
 F28.00 mm  
 F29.00 mm  
 F30.00 mm  
 F31.00 mm  
 F32.00 mm  
 F33.00 mm  
 F34.00 mm  
 F35.00 mm  
 F36.00 mm  
 F37.00 mm  
 F38.00 mm  
 F39.00 mm  
 F40.00 mm  
 F41.00 mm  
 F42.00 mm  
 F43.00 mm  
 F44.00 mm  
 F45.00 mm  
 F46.00 mm  
 F47.00 mm  
 F48.00 mm  
 F49.00 mm  
 F50.00 mm  
 F51.00 mm  
 F52.00 mm  
 F53.00 mm  
 F54.00 mm  
 F55.00 mm  
 F56.00 mm  
 F57.00 mm  
 F58.00 mm  
 F59.00 mm  
 F60.00 mm  
 F61.00 mm  
 F62.00 mm  
 F63.00 mm  
 F64.00 mm  
 F65.00 mm  
 F66.00 mm  
 F67.00 mm  
 F68.00 mm  
 F69.00 mm  
 F70.00 mm  
 F71.00 mm  
 F72.00 mm  
 F73.00 mm  
 F74.00 mm  
 F75.00 mm  
 F76.00 mm  
 F77.00 mm  
 F78.00 mm  
 F79.00 mm  
 F80.00 mm  
 F81.00 mm  
 F82.00 mm  
 F83.00 mm  
 F84.00 mm  
 F85.00 mm  
 F86.00 mm  
 F87.00 mm  
 F88.00 mm  
 F89.00 mm  
 F90.00 mm  
 F91.00 mm  
 F92.00 mm  
 F93.00 mm  
 F94.00 mm  
 F95.00 mm  
 F96.00 mm  
 F97.00 mm  
 F98.00 mm  
 F99.00 mm  
 F100.00 mm

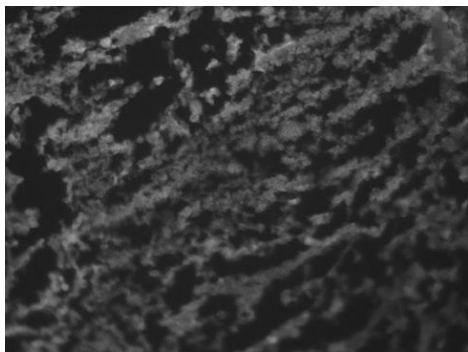
Figure 1 is an axial T2-weighted MRI scan of the abdomen. The image shows a cross-section of the abdominal cavity. A large, well-defined, hyperintense (bright) mass is visible in the upper right quadrant, consistent with the location of the right kidney. The mass has a heterogeneous internal structure. Surrounding organs and structures are visible in various shades of gray. Technical parameters are listed on the left and right sides of the image.

This fluorescence micrograph shows a dense population of cells. The nuclei are stained blue, likely with DAPI. Numerous red puncta are visible throughout the field, indicating the presence of a specific fluorescent marker or protein within the cells.

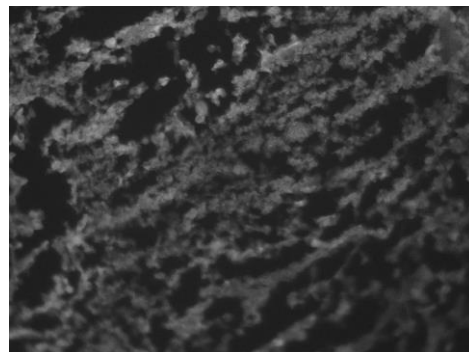


This fluorescence microscopy image shows a cluster of cells. The nuclei are stained blue, and there are numerous red puncta distributed throughout the cell cluster, indicating the presence of a specific marker or protein.

*Figure 3: FISH Images*

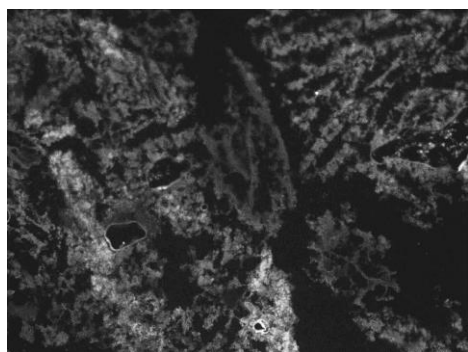


FISCHER 21D\_IC

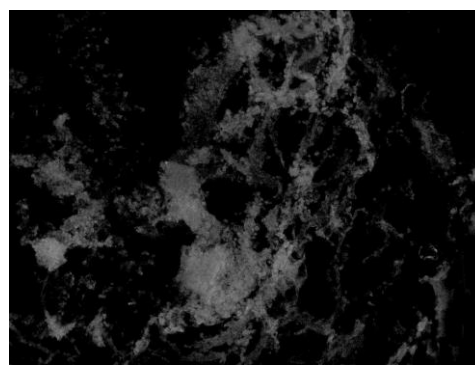


FISCHER 22D\_IV

*Figure 4a: IHC Imaging, Flag*



FISCHER 21C\_IC



FISCHER 24C\_IV

*Figure 4b: IHC Imaging, Hif1- $\alpha$*

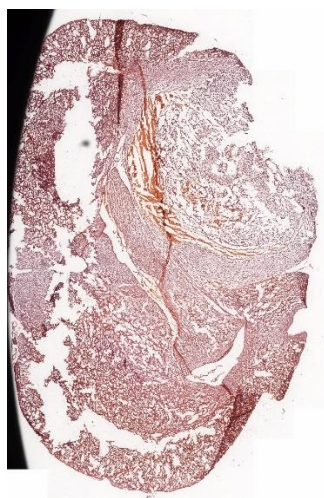
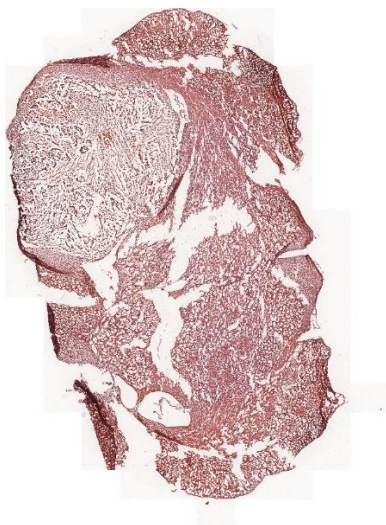


## *Figure 5.H & E Staining*

### **Discussion**

For the first experiment it was successfully shown that sTRAIL protein TRAIL can induce apoptosis on U87MG cells lines in vitro. When the VNP cells, which has the soluble TRAIL plasmid to the tumor cells, are added, the protein is made by bacteria and secreted. Then, TRAIL comes in contact with tumor cells, triggers the apoptosis pathway (similar to your schematic on one of the slides). The DNA gets fragmented and the cells begin to die. Losing their morphology is the first thing that you can see when apoptosis happens. Next, animal studies have to be done to check if TRAIL will induce apoptosis in Glioblastoma cells. For the second experiment, *S. Typhimurium* strain can seek tumors and express Azurin in hypoxic regions. The future plan is to try the xenograft model- U87MG cell lines in athymic rats and inject ST with TRAIL plasmid.

### **References**

1. Falschlehner C, Schaefer U and Walczak H: Following TRAIL's path in the immune system. *Immunol 127: 145-154, 2009.*

2. Wiley SR, Schooley K, Smolak PJ, Din WS, Huang CP, Nicholl JK, Sutherland GR, Smith TD, Rauch C, Smith CA and Goodwin RG: Identification and characterization of a new member of the TNF family that induces apoptosis. *Immunity*
3. Agarwal, M. L., W. R. Taylor, M. V. Chernov, O. B. Chernova, and G. R. Stark. 1998. The p53 network. *J. Biol. Chem.* 273:1–4
4. Gralow J, Ozols RF, Bajorin DF, Cheson BD, Sandler HM, Winer EP, et al. Clinical cancer advances 2007: major research advances in cancer treatment, prevention, and screening – a report from the American Society of Clinical Oncology. *J Clin Oncol* 2008;26(2):313–25.
5. Bauchet L, Rigau V, Mathieu-Daude H, Figarella-Branger D, Hugues D, Palusseau L, et al. French brain tumor data bank: methodology and first results on 10,000 cases. *J Neurooncol* 2007;84(2):189–99.
6. Walker MD, Green SB, Byar DP, Alexander E Jr, Batzdorf U, Brooks WH, Hunt WE, MacCarty CS, Mahaley MS Jr, Mealey J Jr, Owens G, Ransohoff J, Robertson JT, Shapiro WR, Smith KR Jr, Wilson CB, Strike TA. Randomized comparisons of radiotherapy and nitrosoureas for the treatment of malignant glioma after surgery. *N Engl J Med* 1980; 303: 1323–9
7. Stewart LA. Chemotherapy in adult high-grade glioma: a systematic review and meta-analysis of individual patient data from 12 randomised trials. *Lancet* 2002; 359:1011–18
8. Voges, J, Reszka, R, Gossmann, A, et al. Imaging-guided convection-enhanced delivery and gene therapy of glioblastoma. *Annals of Neurology Ann Neurol.* 2003:479–487.
9. Hutchinson, L, Kirk, R. High drug attrition rates—where are we going wrong? *Nature Reviews Clinical Oncology Nat Rev Clin Oncol.* 2011:189–190.

10. Tzakos, AG, Briasoulis, E, Thalhammer, T, Jäger, W, Apostolopoulos, V. Novel Oncology Therapeutics: Targeted Drug Delivery for Cancer. *Journal of Drug Delivery*. 2013:1–5.